International Journal of Innovative
Computing, Information and Control
Volume **20**, Number **3**, June **2024**

ICIC International ©2024 ISSN 1349-4198
pp. **945–963**

ADAPTIVE SUPER-TWISTING CONTROL FOR VIBRATION DISPLACEMENT SYSTEM OF CONTINUOUS CASTING MOLD

Na Yuan[1], Zhuang Ma[1,*], Jian Zhou[2] and Cheng Gong[1]

[1]Key Lab of Intelligent Data Information Processing and Control of Hebei Province
Tangshan University
No. 11, West University Road, Tangshan 063000, P. R. China
yuanna@tsc.edu.cn; gongcheng2004@126.com
*Corresponding author: T0499@tsc.edu.cn

[2]Qingdao Gaoce Technology Co., Ltd.
No. 66, Chongsheng Road, High Tech Zone, Qingdao 266000, P. R. China
zhoujian@henghuiic.com

Received November 2023; revised February 2024

Abstract. *To solve the non-unique problem of inverse solutions of nonlinear periodic function and the uncertainties in the transmission mechanism of vibration displacement system of continuous casting mold driven by servo motor, an adaptive super-twisting control strategy based on nonlinear processing method is proposed. Firstly, a new nonlinear processing method is utilized to solve the problem that the output equation of the system has the non-unique problem of inverse solutions of a nonlinear periodic function, which is convenient for the controller design of displacement loop. Secondly, based on integral non-singular terminal sliding mode, an adaptive super-twisting controller is proposed to suppress the uncertainties including the initial zero position deviation of the eccentric shaft, parameter perturbation, and fast time-varying load disturbance, and track the desired displacement accurately in the displacement loop system. It is proved that the proposed controller can guarantee that all the signals of closed loop system are bounded and can converge to the region near the origin in finite time. Finally, the simulation and experimental researches all verify that the proposed control method is superior to the PI control method in the field and has better dynamic and steady-state tracking performance.*
Keywords: Continuous casting mold, Nonlinear processing method, Sliding mode control, Adaptive control, Finite-time control

1. **Introduction.** Continuous casting is a key part of iron and steel production, and continuous casting mold (CCM) is one part of continuous casting. The non-sinusoidal vibration control of CCM has an important impact on the surface quality and the casting speed of the slab [1,2]. The non-sinusoidal vibration control system of the CCM driven by the servo motor is a new driving mode [3], which is realized by the one-direction and variable speed rotation of the servo motor. Thus, the frequent start and stop of the forward and reverse rotation of the servo motor can be avoided effectively. It has some advantages of energy saving, consumption reduction, compact structure and easy maintenance [4], etc. However, there is a nonlinear periodic function, i.e., sinusoidal function, between the vibration displacement of the mold and the angular displacement of the eccentric shaft in the forward channel of the CCM system. The nonlinear periodic function of the output equation has the non-unique problem of inverse solutions [5], which will bring difficulties to the controller design for tracking the desired vibration displacement. At the same time, there are unknown uncertainties in the CCM system, such as the initial deviation

DOI: 10.24507/ijicic.20.03.945

of eccentric shaft mechanical zero position, parameter perturbation, and varying-time load disturbance, etc., which make it difficult to improve the tracking control accuracy. Therefore, it is necessary to design a closed-loop controller of the vibration displacement loop to improve the tracking accuracy of the vibration displacement system of CCM on the premise of ensuring the stability of the system.

To solve problem of the nonlinear output equation, the piecewise mapping function method was proposed, and mapping relationship between eccentric shaft angular displacement and mold vibration displacement is established in [5-7]. Thus, the problem of vibration displacement tracking can be transformed into the problem of angular displacement tracking, which can simplify the displacement tracking control and facilitate the design of the controller. However, these methods depend on accurate judgment of the extreme points of the CCM vibration displacement system. In industrial practice, due to the influence of sampling time, the judgment condition of the displacement extreme points is only set in a very small neighborhood. However, the range of this neighborhood is difficult to determine, which will lead to inaccurate calculation of the angular displacement of the eccentric shaft. Furthermore, angular displacement of the eccentric shaft increases monotonically because servo motor rotates in one direction, which will lead to data overflow or calculation error due to the long-time operation of the mold. In [8], finite time control of mold vibration displacement was simulated, but no experimental research was carried out, which is one of the main motivations of this study.

For the uncertainty suppression problem of nonlinear control system, many research results have been achieved. In [9,10], feedback linearization and proportional-integral (PI) control were used to deal with the above problems. However, finite time stability cannot be achieved under the above methods. Compared to traditional asymptotic stability, the finite time stability can better characterize the transient behavior of a system within a specific time interval. Due to its ability to ensure finite time stability and strong robustness, sliding mode control is widely used in various control fields [11]. However, chattering is a common problem in traditional sliding mode control (SMC) [12,13]. Moreover, high-order sliding mode control (HOSMC) not only retains the advantages of the traditional SMC but also reduces the chattering problem, which can improve the control accuracy of the SMC system and eliminate the limitation of relative order. Therefore, HOSMC has become a research hotspot in recent years [14-17]. Particularly, super-twisting SMC is one kind of HOSMC, and suppresses the chattering phenomenon effectively. The derivative information of sliding mode variables is not needed and the control law is continuous [18,19]. In [20], a new saturated super-twisting algorithm is proposed and applied to the design of missile guidance law against a highly maneuvering target whose maneuvering acceleration is very close to that of the missile or even exceeds the missile normal acceleration in a finite period of time. To solve the problem of speed pulsation in a single-winding magnetic levitation switched reluctance motor system, a super-twisting SMC controller was designed in [21], and the dynamic characteristics and robustness of the system were improved. However, the above methods need to know the upper bound of the disturbance derivative, but in many cases, the upper bound is difficult to obtain [18]. To solve this problem, a parameter adaptive algorithm based super twisted SMC was proposed in [22-24]. However, the algorithm needs to assume that the uncertainty of the system meets certain limit conditions, which increases the difficulty of the system control.

Based on the above analysis, to solve the nonlinear output equation and unknown disturbances of the CCM displacement tracking control system, a nonlinear processing method and an adaptive super-twisting control strategy are proposed in this paper. Firstly, aiming at the problem that the output equation is nonlinear, a novel piecewise mapping method is designed. Under the proposed method, the mapping relationship between

eccentric shaft angular displacement tracking error and mold vibration displacement is established without judging the extreme point of CCM vibration displacement, which can simplify the system model, and facilitate the design of the controller. Secondly, to suppress the influence of uncertainties of the CCM system and improve the tracking control accuracy of mold vibration displacement, combined with integral non-singular terminal sliding mode and adaptive super-twisting algorithm, an adaptive controller is proposed without knowing the upper bound of disturbance derivative. And then, it is proved that the tracking error of the CCM vibration displacement can converge to the region near the origin in finite time by Lyapunov stability theory. Finally, the effectiveness of the proposed method is proved by simulation and experimental research.

This paper is organized as follows. Section 2 presents the mathematical model of the CCM vibration displacement system and a nonlinear processing method to simplify the controller design. And then, an adaptive sliding mode control based on super-twisting is designed and its finite-time stability is proved in Section 3. Simulation and experimental results are presented to verify the effectiveness of the proposed method in Section 4. Finally, the conclusion of the article is given in Section 5.

2. Mathematical Model of CCM System and Nonlinear Processing Method.

2.1. Mathematical model and problem descriptions. In this paper, the vibration displacement control system of the CCM driven by a servo motor is shown in Figure 1(a).

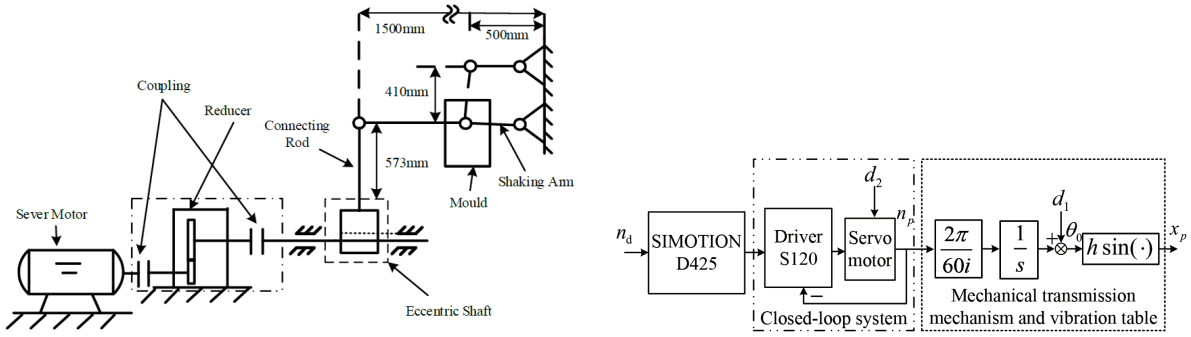

(a) Schematic diagram of simulation shaking flat (b) Control schematic diagram

FIGURE 1. Schematic diagram of simulation shaking flat and control vibration system of CCM driven by a servo motor

The working principle of the CCM system is that the servo motor rotates through variable speed or constant speed with one direction, and drives the mold through a reducer, an eccentric shaft, and some linkage mechanisms to realize non-sinusoidal or sinusoidal vibration. Moreover, the experimental device used in this paper is a CCM simulation shaking table based on SIMOTION D425, which is one kind of high-performance motion controller. In addition, the closed-loop PI control of the servo motor current loop and speed loop is realized by servo driver S120, which is shown in Figure 1(b). To simplify controller design and the experimental research, the closed-loop control system can be approximated as a second-order oscillation system, and the form is

$$\frac{n_p(s)}{n_d(s)} = \frac{K}{T^2 s^2 + 2\xi T s + 1} \tag{1}$$

where $n_p(s)$ and $n_d(s)$ are the actual speed and the given speed of the motor, respectively. ξ is the damping ratio. K and T are the gain and the time constant of the closed-loop system.

Furthermore, considering the initial deviation of mechanical zero position of the eccentric shaft, the deviation between the identification model of the motor closed-loop system and the actual model, the time varying load torque and other disturbances, the mathematical model can be established as [3].

$$\begin{cases} \dot{x}_p = h\dfrac{2\pi n_p}{60i}\cos\left(\displaystyle\int_{t_0}^{t}\frac{2\pi n_p}{60i}d\tau + d_1\right) \\ \ddot{n}_p = -\dfrac{1}{T^2}n_p - \dfrac{2\xi}{T}\dot{n}_p + \dfrac{K}{T^2}n_d + d_2 \end{cases} \tag{2}$$

where x_p is the actual vibration displacement of the CCM, h is the vibration amplitude of the CCM, i is the reduction ratio, d_1 and d_2 are the initial zero phases offset of the eccentric shaft with a constant number and the compound disturbances, respectively. In detail, the compound disturbances include the deviation between the motor closed-loop system identification model and the actual model and the time-varying load disturbance.

In summary, the control objective of this paper is to design a controller to suppress the compound disturbances and track the desired displacement. However, the system output equation is a nonlinear equation, i.e., $x_p = h\sin\left(\int_{t_0}^{t}\frac{2\pi n_p}{60i}d\tau + d_1\right)$ and it is complicated, which brings great difficulties to the controller design. Therefore, the problem of the nonlinear output equation is to be solved firstly and then the controller is designed to realize the accurate tracking control of mold vibration displacement.

The following assumptions and lemmas are used in the designing and stability proof of the closed loop system.

Assumption 2.1. *In the closed-loop control system of the CCM vibration displacement, the phase difference between x_p and x_d is less than $\pi/2$, where x_d is the desired vibration displacement of the CCM.*

Remark 2.1. *In the closed-loop control of mold vibration displacement system, the phase error between the actual mold vibration displacement x_p and its expected trajectory x_d is very small, which can meet Assumption 2.1.*

Assumption 2.2. *The unknown perturbation d is differentiable, and it satisfies*

$$\left|\dot{d}\right| \le \eta, \quad \forall t \ge 0 \tag{3}$$

where $\eta > 0$ is an unknown constant.

Lemma 2.1. [25] *For the nonlinear system*

$$\dot{x} = f(x) \quad f(0) = 0, \quad x \in R^n \tag{4}$$

Suppose $V(x)$ is a continuously differentiable function, and it satisfies the following.

1) $V(x)$ is a positive definite function.

2) There exist positive real numbers $\varepsilon > 0$, $0 < \eta < \infty$ and $\kappa \in (0, 1)$, and the following formula is satisfied with

$$\dot{V}(x) \le -\varepsilon V(x)^{\kappa} + \eta \tag{5}$$

Then the system (4) is practically finite-time stable. Namely, the trajectory of x enters the invariant set given by $x \in \left\{V^{\kappa}(x) \le \frac{\eta}{\varepsilon(1-\beta)}\right\}$, and its convergence time T_0 is satisfied

$$T_0 \le \frac{V^{1-\kappa}(x_0)}{\varepsilon\beta(1-\kappa)} \tag{6}$$

where $0 < \beta < 1$.

Lemma 2.2. [26] *For any positive constants m, n, w and any variables φ, ψ, one has*

$$|\varphi|^m|\psi|^n \leq \frac{m}{m+n}w|\varphi|^{m+n} + \frac{n}{m+n}w^{-\frac{m}{n}}|\psi|^{m+n} \tag{7}$$

2.2. **Nonlinear processing method of mold vibration displacement system.** To solve the problem that the output equation of the CCM system is a nonlinear equation, a piecewise mapping processing method is proposed in this section.

The mapping relationship between eccentric shaft angular displacement tracking error and mold vibration displacement is established, which can simplify the system model. Under the piecewise mapping processing method, the design of displacement tracking controller is facilitated, and the judgment of extreme point of mold vibration displacement is not needed. Therefore, it is easy to be applied to the practical engineering system.

Define $\theta_p = \arcsin(x_p/h)$ and $\theta_d = \arcsin(x_d/h)$ as the actual and desired angular displacement of the eccentric shaft, and the relationship between θ_p and x_p is $x_p = h\sin(\theta_p)$, which is shown in Figure 1(b); x_d the desired vibration displacement of the CCM and the relationship between θ_d and x_d is $x_d = h\sin(\theta_d)$. Moreover, it is seen that x_d can also be accurately tracked by x_p if θ_d can be accurately tracked by θ_p. Therefore, the displacement tracking problem of the CCM system can be transformed into the angular displacement tracking problem of the eccentric shaft.

Theorem 2.1. *Suppose that Assumption 2.1 is satisfied, then the tracking error $\Delta\theta$ of the angular displacement of the eccentric shaft, i.e., $\Delta\theta = \theta_p - \theta_d$, is continuous and satisfies as the following*

$$\Delta\theta = \begin{cases} (\theta_p - \theta_d)\mathrm{sgn}(v_p) & v_p v_d > 0 \\ (\theta_p - \theta_d)\mathrm{sgn}(v_p)\mathrm{sgn}(v_d) & v_p v_d = 0 \\ (\theta_p + \theta_d - \pi\mathrm{sgn}(x_d))\mathrm{sgn}(v_p) & v_p v_d < 0 \end{cases} \tag{8}$$

where v_p and v_d are the actual and desired vibration speed signals of the CCM displacement system, respectively. $\mathrm{sgn}(\cdot)$ *is the signal function as the following*

$$\mathrm{sgn}(\gamma) = \begin{cases} 1 & \gamma \geq 0 \\ -1 & \gamma < 0 \end{cases}, \quad \gamma \in R \tag{9}$$

Proof: In the practical system, x_p actually lags behind x_d. And combining with the analysis of the CCM vibration model, one vibration period is taken as an example in Figure 2. c_1 and c_2 are the points which the difference between the value θ_d and θ_p is

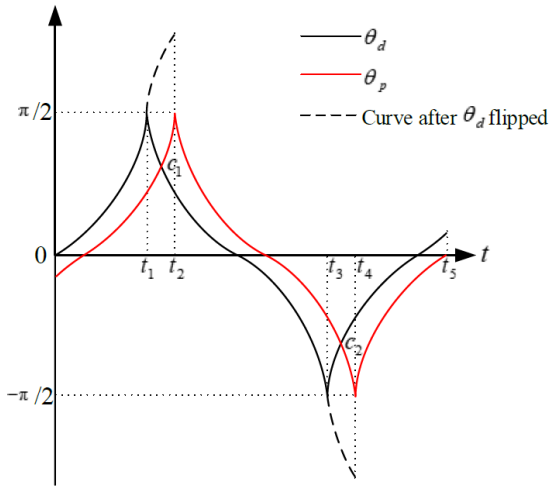

FIGURE 2. Schematic diagram of the nonlinear processing method

zero. t_1 and t_3 are the points with $v_d = 0$. t_2 and t_4 are the points with $v_p = 0$. t_5 is the point with $\theta_p = 0$.

1) When $v_p v_d > 0$, $\Delta\theta$ can be expressed as

$$\Delta\theta = \begin{cases} (\theta_p - \theta_d) \times 1 & v_p > 0,\ v_d > 0,\ t \in [0, t_1) \\ (\theta_p - \theta_d) \times (-1) & v_p < 0,\ v_d < 0,\ t \in (t_2, t_3) \\ (\theta_p - \theta_d) \times 1 & v_p > 0,\ v_d > 0,\ t \in (t_4, t_5] \end{cases} \tag{10}$$

where 1 and -1 can be replaced to $\mathrm{sgn}(v_p)$, and thus the error expression $\Delta\theta$ can be simplified as

$$\Delta\theta = (\theta_p - \theta_d)\mathrm{sgn}(v_p) \tag{11}$$

2) When $v_p v_d = 0$, $\Delta\theta$ can be expressed as

$$\Delta\theta = \begin{cases} (\theta_p - \theta_d) \times 1 & v_p > 0,\ v_d = 0,\ t = t_1 \\ (\theta_p - \theta_d) \times (-1) & v_p = 0,\ v_d < 0,\ t = t_2 \\ (\theta_p - \theta_d) \times (-1) & v_p < 0,\ v_d = 0,\ t = t_3 \\ (\theta_p - \theta_d) \times 1 & v_p = 0,\ v_d > 0,\ t = t_4 \end{cases} \tag{12}$$

where 1 and -1 can be replaced by $\mathrm{sgn}(v_d)\mathrm{sgn}(v_p)$, and then the error expression $\Delta\theta$ can be simplified as

$$\Delta\theta = (\theta_p - \theta_d)\mathrm{sgn}(v_d)\mathrm{sgn}(v_p) \tag{13}$$

3) When $v_p v_d < 0$, $\Delta\theta$ is obtained as the direct difference between θ_d and θ_p, which cannot reflect the angular displacement error of the eccentric shaft. The following is an example: the difference between the value θ_d of the point c_1 and the value θ_p of the point c_2 is zero shown in Figure 2, but the actual displacement of the mold at these two points lags behind the desired displacement. The angular error of the eccentric shaft is not zero. Thus, $\theta_d(\theta_p) = \pm\pi/2$ is flipped as the axis of symmetry when $v_p v_d < 0$, and the value obtained after flipping is $\pi - \theta_d$ ($\theta_n > 0$, $\theta_{rn} > 0$) or $-\pi - \theta_{rn}$ ($\theta_n < 0$, $\theta_{rn} < 0$) as shown by the dotted line in Figure 2. Then $\Delta\theta$ can be expressed as

$$\Delta\theta = \begin{cases} (\theta_p - (\pi - \theta_d)) \times 1 & v_p > 0, v_d < 0, t \in (t_1, t_2) \\ (\theta_p - (-\pi - \theta_d)) \times (-1) & v_p < 0, v_d > 0, t \in (t_3, t_4) \end{cases} \tag{14}$$

where the symbols of the total expression and the item π are replaced by $-\mathrm{sgn}(x_d)$ and $\mathrm{sgn}(v_p)$, respectively. Then $\Delta\theta$ can be expressed as

$$\Delta\theta = (\theta_p + \theta_d - \pi\mathrm{sgn}(x_d))\mathrm{sgn}(v_p) \tag{15}$$

Therefore, Formula (8) is obtained from Formulas (11), (13) and (15).

The $\Delta\theta$ continuity analysis is as the following.

1) Continuity analysis under $v_p v_d > 0$ and $v_p v_d < 0$

In Figure 2, $\Delta\theta$ is also continuous because θ_p and θ_d are continuous. Therefore, it is only necessary to prove the continuity at the flipped time $t = t_1$, $t = t_2$, etc.

2) Continuity analysis at the flipping points

According to Figure 2, the flipped points include four points in a period, and these points are $t = t_1$, $t = t_2$, $t = t_3$ and $t = t_4$, respectively. Therefore, only two points ($t = t_1$, $t = t_2$) need to be analyzed because the two points are the same.

a) Continuity analysis at $t = t_1$:

The left limit of $\Delta\theta$ at $t = t_1$ is

$$\lim_{t \to t_1^-} \Delta\theta = \theta_p - \theta_d \tag{16}$$

At the same time, the right limit of $\Delta\theta$ at $t = t_1$ is

$$\lim_{t\to t_1^+} \Delta\theta = \theta_p - \lim_{t\to t_1^+} (\pi - \theta_d) = \theta_p - \theta_d \tag{17}$$

And the value $\Delta\theta$ at $t = t_1$ is

$$\Delta\theta(t = t_1) = \theta_p - \theta_d \tag{18}$$

From Formulas (16), (17) and (18), the result is obtained.

$$\lim_{t\to t_1^-} \Delta\theta = \lim_{t\to t_1^+} \Delta\theta = \Delta\theta(t = t_1) \tag{19}$$

Therefore, $\Delta\theta$ is continuous at $t = t_1$.

b) Continuity analysis at $t = t_2$:

The left limit of $\Delta\theta$ at $t = t_2$ is

$$\lim_{t\to t_2^-} \Delta\theta = \theta_n - \lim_{t\to t_2^-} (\pi - \theta_d) = \theta_p - (\theta_p + (\theta_p - \theta_d)) = (\theta_p - \theta_d) \times (-1) \tag{20}$$

And the right limit of $\Delta\theta$ at $t = t_2$ is

$$\lim_{t\to t_2^+} \Delta\theta = (\theta_p - \theta_d) \times (-1) \tag{21}$$

In addition, the value $\Delta\theta$ at $t = t_2$ is

$$\Delta\theta(t = t_2) = (\theta_p - \theta_d) \times (-1) \tag{22}$$

From Formulas (20), (21) and (22), the result is obtained.

$$\lim_{t\to t_2^-} \Delta\theta = \lim_{t\to t_2^+} \Delta\theta = \Delta\theta(t = t_2) \tag{23}$$

Therefore, $\Delta\theta$ is continuous at $t = t_2$.

Remark 2.2. *From the above analysis, it can be proved that $\Delta\theta$ is also continuous at other flipping points. When the actual displacement of the CCM system is ahead of the given displacement, it can be proved by the same method.*

Define $x_1 = \theta_p$, $x_2 = n_p$, $x_3 = \dot{n}_p$, and then the mathematical model (2) of the CCM vibration can be equivalently simplified as

$$\begin{cases} \dot{x}_1 = \dfrac{2\pi}{60i} x_2 \\ \dot{x}_2 = x_3 \\ \dot{x}_3 = -\dfrac{1}{T^2} x_2 - \dfrac{2\xi}{T} x_3 + \dfrac{K}{T^2} u + d_2 \end{cases} \tag{24}$$

where $u = n_r$, n_r is the expected speed of the servo motor.

Remark 2.3. *In the closed-loop control of the CCM vibration displacement system, the phase difference is very small, which is satisfied with Assumption 2.1. Thus, the different symbols of θ_p and θ_d will not occur when $v_p v_d < 0$.*

3. Adaptive Super-Twisting SMC Controller Design.

In this section, an adaptive super-twisting SMC controller is designed to improve the tracking accuracy and anti-interrupt ability of vibration displacement of the CCM.

3.1. Nominal continuous control v_{nom}.

Define the tracking error of the angular displacement as

$$e = \Delta\theta = x_1 - \theta_d \tag{25}$$

Let $z_1 = e$, $z_2 = \dot{z}_1$, $z_3 = \dot{z}_2$, and then Formula (24) can be transformed into the form of the following error model.

$$\begin{cases} \dot{z}_1 = z_2 \\ \dot{z}_2 = z_3 \\ \dot{z}_3 = f(z) + gu + d \end{cases} \tag{26}$$

where $g = \frac{K\pi}{30T^2 i}$, $d = \frac{\pi}{30i} d_2$, $f(z) = -\frac{1}{T^2} z_2 - \frac{2\xi}{T} z_3 - \frac{1}{T^2}\dot{\theta}_d - \frac{2\xi}{T}\ddot{\theta}_d - \dddot{\theta}_d$.

For the error model (26), the feedback control law is designed as

$$u = \frac{1}{g}(-f(z) + \upsilon) \tag{27}$$

where υ includes a nominal control item υ_{nom} and a robust control item υ_{st} [13], and υ is designed as the following.

$$\upsilon = \upsilon_{nom} + \upsilon_{st} \tag{28}$$

Note the nominal control item υ_{nom} can make the nominal system converge to the region near the origin in finite time, and the control item υ_{st} is a super-twisting algorithm control item, which can reduce the chattering and enhance the system robustness. The design of υ_{nom} and υ_{st} will be given later.

Combining Formula (27), Formula (26) is rewritten as

$$\begin{cases} \dot{z}_1 = z_2 \\ \dot{z}_2 = z_3 \\ \dot{z}_3 = \upsilon + d \end{cases} \tag{29}$$

Define variables as $\xi_1 = z_1$, $\xi_2 = z_2 - \alpha_1$, $\xi_3 = z_3 - \alpha_2$, where α_1 and α_2 are the virtual control laws to be designed later. According to the backstepping control method, the nominal control item υ_{nom} is designed as

$$\upsilon_{nom} = -\xi_2 + \dot{\alpha}_2 - \frac{1}{2}\xi_3 - c_3 sig^l(\xi_3) \tag{30}$$

where $\alpha_1 = -c_1 sig^l(\xi_1)$, $\alpha_2 = -\xi_1 + \dot{\alpha}_1 - c_2 sig^l(\xi_2)$, $0 < l < 1$, $c_1 > 0$, $c_2 > 0$, $c_3 > 0$ are constants.

The proof process will be given later.

3.2. **Adaptive super-twisting SMC control.** In this section, to improve the anti-interrupt ability of the system while $d \neq 0$, an adaptive super-twisting SMC controller based on super-twisting algorithm is designed, which can impel the system states convergence to the origin in finite time and improve the tracking control accuracy and the robustness of the system.

Define s as a sliding mode surface variable

$$s = z_3 - \int_{t_0}^{t} \upsilon_{nom} d\tau \tag{31}$$

Combining with Formulas (28) and (29), the derivative of s is

$$\dot{s} = \dot{z}_3 - \upsilon_{nom} = \upsilon + d - \upsilon_{nom} = \upsilon_{st} + d \tag{32}$$

For the system (32), $s \to 0$ can be realized in finite time with the traditional first-order SMC $\upsilon_{st} = -k\mathrm{sgn}(s)$ with $k > 0$. However, due to the existence of the high-frequency switching term $-k\mathrm{sgn}(s)$, the chattering phenomenon of the traditional SMC is very serious. Generally, the super-twisting SMC algorithm can effectively suppress the chattering phenomenon and improve the robustness of the system. Thus, the second-order sliding mode is adopted, and the form of the adaptive super-twisting SMC algorithm is as follows:

$$\begin{cases} \upsilon_{st} = -k_1|s|^{\frac{1}{2}}\text{sgn}(s) + \varsigma \\ \dot{\varsigma} = -k_2\text{sgn}(s) \end{cases} \tag{33}$$

where ς is the state variable of super-twisting SMC, $k_2 = \rho + \frac{\vartheta^2}{4} + \frac{k_1\vartheta}{4}$, k_1 is adaptive parameter, and the adaptive law is

$$\dot{k}_1 = \begin{cases} |s|^{-\frac{1}{2}}j_1^2 - k_1 & s \neq 0 \\ 0 & s = 0 \end{cases} \tag{34}$$

where ρ and ϑ are all positive constants with $\vartheta > 3$.

Theorem 3.1. *For the system (26), if Assumption 2.2 is satisfied, adaptive law is (34) and the adaptive super-twisting SMC controller is designed as*

$$u = \frac{1}{g}(-f(z) + \upsilon_{nom} + \upsilon_{st}) \tag{35}$$

Then the states of the system (26) are convergent to the neighborhood near the origin in finite time.

Proof: Define variable χ as

$$\chi = d - k_2\int_{t_0}^{t}\text{sgn}(s)d\tau \tag{36}$$

Substitute Formula (33) into Formula (32) and combining with Formula (36), Formula (32) is rewritten as

$$\begin{cases} \dot{s} = -k_1|s|^{\frac{1}{2}}\text{sgn}(s) + \chi \\ \dot{\chi} = -k_2\text{sgn}(s) + \dot{d} \end{cases} \tag{37}$$

The vector $j = [j_1, j_2]^T = \left[\text{sgn}(s)|s|^{\frac{1}{2}}, \chi\right]^T$ is taken, then

$$\begin{cases} \dot{j}_1 = \dfrac{1}{2|s|^{\frac{1}{2}}}\left(-k_1|s|^{\frac{1}{2}}\text{sgn}(s) + \chi\right) \\ \dot{j}_2 = -k_2\text{sgn}(s) + \dot{d} \end{cases} \tag{38}$$

Let $\tilde{\dot{d}} = |s|^{\frac{1}{2}}\dot{d}$, $A = \begin{pmatrix} -\frac{k_1}{2} & \frac{1}{2} \\ -k_2 & 0 \end{pmatrix}$, $B = [0, 1]^T$, and Formula (37) is rewritten as

$$j = |s|^{-\frac{1}{2}}\left(Aj + B\tilde{\dot{d}}\right) \tag{39}$$

A Lyapunov candidate function is selected as

$$V(j, k_1) = V_0(j) + \frac{1}{2}\left(2\rho + \frac{\vartheta^2}{4}\right)(k_1 - k_1^*)^2 \tag{40}$$

where k_1^* is a positive constant, $V_0(j) = j^TPj$, P is a positive definite matrix and defined as $P = \frac{1}{2}\begin{pmatrix} 4\rho + \vartheta^2 & -\vartheta \\ -\vartheta & 2 \end{pmatrix}$.

Taking the derivative of $V_0(j)$, it can be obtained that

$$\begin{aligned} &\dot{V}_0(j) \\ &= |s|^{-\frac{1}{2}}j^T\left(A^TP + PA\right)j + 2|s|^{-\frac{1}{2}}j^TPB\tilde{\dot{d}} \\ &\leq |s|^{-\frac{1}{2}}j^T\left(A^TP + PA\right)j + |s|^{-\frac{1}{2}}j^TPBB^TPj + |s|^{-\frac{1}{2}}\tilde{\dot{d}}^2 \\ &\leq |s|^{-\frac{1}{2}}j^T\left(A^TP + PA\right)j + |s|^{-\frac{1}{2}}j^TPBB^TPj + |s|^{-\frac{1}{2}}\tilde{\dot{d}}^2 + \eta^2|s|^{-\frac{1}{2}}j^TC^TCj - |s|^{-\frac{1}{2}}\tilde{\dot{d}}^2 \end{aligned}$$

$$= |s|^{-\frac{1}{2}} j^T \left(A^T P + PA + PBB^T P + \eta^2 C^T C\right) j \tag{41}$$

where $C = [1, 0]$.

According to the defining of A, B, C and P, we can have

$$A^T P + PA + PBB^T P + \eta^2 C^T C = -W \tag{42}$$

where $W = \begin{pmatrix} W_{11} & W_{12} \\ W_{21} & \frac{\tau}{2} - 1 \end{pmatrix}$, $W_{11} = 2k_1\rho + \frac{k_1\vartheta^2}{2} - k_2\vartheta - \eta^2 - \frac{\vartheta^2}{4}$, $W_{12} = W_{21} = -\rho - \frac{\vartheta^2}{4} - \frac{k_1\vartheta}{4} + k_2 + \frac{\vartheta}{2}$.

According to $k_2 = \rho + \frac{\vartheta^2}{4} + \frac{k_1\vartheta}{4}$, we can have

$$W = \begin{pmatrix} W_{11} & \frac{\vartheta}{2} \\ \frac{\vartheta}{2} & \frac{\vartheta}{2} - 1 \end{pmatrix} \tag{43}$$

Substituting Formulas (42) and (43) into Formula (41), then we can obtain that

$$\begin{aligned} \dot{V}_0(j) &= -|s|^{-\frac{1}{2}} j^T W j \\ &= |s|^{-\frac{1}{2}} \left(-W_{11} j_1^2 - \vartheta j_1 j_2 - \left(\frac{\vartheta}{2} - 1\right) j_2^2\right) \\ &\leq |s|^{-\frac{1}{2}} \left(-\left(W_{11} - \frac{\vartheta}{2}\right) j_1^2 - \frac{\vartheta - 3}{2} j_2^2\right) \end{aligned} \tag{44}$$

Defining $k_1^* = \frac{\rho\vartheta + \frac{\vartheta^3}{4} + \eta^2 + \frac{3\vartheta^2}{4} + \delta}{2\rho + \frac{\vartheta^2}{4}}$, we can know $-\left(W_{11} - \frac{\vartheta}{2}\right) + \delta = -\left(2\rho + \frac{\vartheta^2}{4}\right)(k_1 - k_1^*)$, where $\delta > 0$ is a constant. According to Formula (44), it can be obtained that

$$\begin{aligned} \dot{V}_0(j) &\leq |s|^{-\frac{1}{2}} \left(-\left(W_{11} - \frac{\vartheta}{2} - \delta\right) j_1^2 - \delta j_1^2 - \frac{\vartheta - 3}{2} j_2^2\right) \\ &= |s|^{-\frac{1}{2}} \left(-\left(2\rho + \frac{\vartheta^2}{4}\right)(k_1 - k_1^*) j_1^2 - \delta j_1^2 - \frac{\vartheta - 3}{2} j_2^2\right) \end{aligned} \tag{45}$$

According to Formula (45), the derivative of $V(j, k_1)$ is as the following.

$$\begin{aligned} \dot{V}(j, k_1) &\leq |s|^{-\frac{1}{2}} \left(-\left(2\rho + \frac{\vartheta^2}{4}\right)(k_1 - k_1^*) j_1^2 - \delta j_1^2 - \frac{\vartheta - 3}{2} j_2^2\right) + \left(2\rho + \frac{\vartheta^2}{4}\right)(k_1 - k_1^*) \dot{k}_1 \\ &= |s|^{-\frac{1}{2}} \left(-\delta j_1^2 - \frac{\vartheta - 3}{2} j_2^2\right) + \left(2\rho + \frac{\vartheta^2}{4}\right)(k_1 - k_1^*) \left(-|s|^{-\frac{1}{2}} j_1^2 + \dot{k}_1\right) \end{aligned} \tag{46}$$

Substituting Formula (34) into Formula (46), then we can obtain that

$$\begin{aligned} \dot{V}(j, k_1) \leq\ & |s|^{-\frac{1}{2}} \left(-\delta j_1^2 - \frac{\vartheta - 3}{2} j_2^2\right) - \left(2\rho + \frac{\vartheta^2}{4}\right)(k_1 - k_1^*) k_1 \\ & + \left(\frac{1}{2}\left(2\rho + \frac{\vartheta^2}{4}\right)(k_1 - k_1^*)^2\right)^{\frac{1}{2}} - \left(\frac{1}{2}\left(2\rho + \frac{\vartheta^2}{4}\right)(k_1 - k_1^*)^2\right)^{\frac{1}{2}} \end{aligned} \tag{47}$$

According to Young's inequality, it can be obtained that

$$\begin{aligned} -\left(2\rho + \frac{\vartheta^2}{4}\right)(k_1 - k_1^*) k_1 &= -\left(2\rho + \frac{\vartheta^2}{4}\right)(k_1 - k_1^*)^2 - \left(2\rho + \frac{\vartheta^2}{4}\right)(k_1 - k_1^*) k_1^* \\ &\leq -\frac{1}{2}\left(2\rho + \frac{\vartheta^2}{4}\right)(k_1 - k_1^*)^2 + \frac{1}{2}\left(2\rho + \frac{\vartheta^2}{4}\right)(k_1^*)^2 \end{aligned} \tag{48}$$

According to Lemma 2.2, we can get

$$\left(\frac{1}{2}\left(2\rho+\frac{\vartheta^2}{4}\right)(k_1-k_1^*)^2\right)^{\frac{1}{2}} \leq \frac{1}{4}+\frac{1}{2}\left(2\rho+\frac{\vartheta^2}{4}\right)(k_1-k_1^*)^2 \tag{49}$$

Substituting Formulas (48) and (49) into Formula (47), then we can obtain that

$$\begin{aligned}
&\dot{V}(j,k_1)\\
&\leq |s|^{-\frac{1}{2}}\left(-\delta j_1^2-\frac{\vartheta-3}{2}j_2^2\right)-\left(\frac{1}{2}\left(2\rho+\frac{\vartheta^2}{4}\right)(k_1-k_1^*)^2\right)^{\frac{1}{2}}+\frac{1}{2}\left(2\rho+\frac{\vartheta^2}{4}\right)(k_1^*)^2+\frac{1}{4}\\
&\leq -r_0|s|^{-\frac{1}{2}}\left(j_1^2+j_2^2\right)-\left(\frac{1}{2}\left(2\rho+\frac{\vartheta^2}{4}\right)(k_1-k_1^*)^2\right)^{\frac{1}{2}}+r_1
\end{aligned} \tag{50}$$

where $r_0=\min\left\{\delta,\frac{\vartheta-3}{2}\right\}$, $r_1=\frac{1}{2}\left(2\rho+\frac{\vartheta^2}{4}\right)(k_1^*)^2+\frac{1}{4}$.

According to $\|j\|_2^2=j_1^2+j_2^2$, we can have $\|j\|_2\geq|j_1|$; According to $|j_1|=|s|^{\frac{1}{2}}$, it can be obtained that

$$|s|^{-\frac{1}{2}}\geq\|j\|_2^{-1} \tag{51}$$

Substituting Formula (51) into Formula (50), then we can know

$$\begin{aligned}
\dot{V}(j,k_1)&\leq -r_0|s|^{-\frac{1}{2}}\|j\|_2^2-\left(\frac{1}{2}\left(2\rho+\frac{\vartheta^2}{4}\right)(k_1-k_1^*)^2\right)^{\frac{1}{2}}+r_1\\
&\leq -r_0\|j\|_2-\left(\frac{1}{2}\left(2\rho+\frac{\vartheta^2}{4}\right)(k_1-k_1^*)^2\right)^{\frac{1}{2}}+r_1\\
&\leq -r_2V^{\frac{1}{2}}(j,k_1)+r_1
\end{aligned} \tag{52}$$

where $r_2=\min\left\{r_0\lambda_{\max}^{-\frac{1}{2}}(P)\right\}$.

According to Lemma 2.1, it is shown that j_1 and j_2 can converge to the neighborhood near the origin in finite time and the convergent time t_F is satisfied with

$$t_F\leq\frac{2V^{\frac{1}{2}}(t_0)}{r_2\beta_0} \tag{53}$$

where $0<\beta_0<1$, t_0 is the initial time.

When $t>t_F$, the sliding mode s and $\dot{s}$ can converge to the neighborhood near the origin in finite time, and there exists a constant $c_s>0$ that satisfies $|\dot{s}|\leq c_s$. Thus, we can have $\dot{z}_3=\upsilon_{nom}+\dot{s}$.

Selecting $V_1=\frac{1}{2}\xi_1^2$, according to $\alpha_1=-c_1sig^l(\xi_1)$, it can be obtained that

$$\dot{V}_1=\xi_1(\xi_2+\alpha_1)=-c_1|\xi_1|^{l+1}+\xi_1\xi_2 \tag{54}$$

Selecting $V_2=V_1+\frac{1}{2}\xi_2^2$, according to $\alpha_2=-\xi_1+\dot{\alpha}_1-c_2sig^l(\xi_2)$, it can be obtained that

$$\dot{V}_2=\dot{V}_1+\xi_2(z_3-\dot{\alpha}_1)=-c_1|\xi_1|^{l+1}-c_2|\xi_2|^{l+1}+\xi_2\xi_3 \tag{55}$$

Selecting $V_3=V_2+\frac{1}{2}\xi_3^2$, according to (30), it can be obtained that

$$\begin{aligned}
\dot{V}_3&=\dot{V}_2+\xi_3(\upsilon_{nom}+\dot{s}-\dot{\alpha}_2)\\
&=-c_1|\xi_1|^{l+1}-c_2|\xi_2|^{l+1}-c_3|\xi_3|^{l+1}-\frac{1}{2}\xi_3^2+\xi_3\dot{s}\\
&\leq -c_1|\xi_1|^{l+1}-c_2|\xi_2|^{l+1}-c_3|\xi_3|^{l+1}-\frac{1}{2}\xi_3^2+\frac{1}{2}\xi_3^2+\frac{1}{2}\dot{s}^2
\end{aligned}$$

$$\leq -\bar{c}V_3^{\frac{l+1}{2}} + \frac{1}{2}c_s^2 \tag{56}$$

where $\bar{c} = \min\{c_1, c_2, c_3\}$.

According to Lemma 2.1, it is shown that ξ_1, ξ_2 and ξ_3 can converge to the neighborhood near the origin in finite time and the convergent time t_r is satisfied with

$$t_r \leq \frac{2V_3^{1-\frac{l+1}{2}}(t_F)}{\bar{c}\beta_1\left(1-\frac{l+1}{2}\right)} \tag{57}$$

where $0 < \beta_1 < 1$.

It can be seen that the states of the system (26) can converge to the neighborhood near the origin in finite time $T = t_F + t_r$.

Remark 3.1. *Considering that the CCM vibration displacement system is difficult to strictly converge to zero and fluctuates in small neighborhoods close to zero, the parameter adaptive laws (34) make k_1 increasing continuously, which may lead to the instability of the system. Therefore, the convergence conditions can be relaxed appropriately to make it convergence to the neighborhood near the origin, and the parameter adaptive law is designed as [19]*

$$\dot{k}_1 = \begin{cases} \left(|s|^{-\frac{1}{2}}j_1^2 - k_1\right) sign(|s| - \mu), & k_1 > k_m \\ \varphi, & k_1 \leq k_m \end{cases} \tag{58}$$

where μ, k_m and φ are all positive constants, $\mu < \gamma$.

4. Simulation and Experimental Researches.

4.1. Simulation researches.

In this section, the proposed control strategy is simulated. Due to its ability to effectively improve controller response speed and reduce system steady-state errors, PI control is acceptable and widely used in many practical applications. However, PI control is insensitive to external disturbances in the system and can only ensure asymptotic stability of the system state. In order to further demonstrate the effectiveness of the proposed controller, a simulation comparison is conducted between the proposed controller and the PI controller. In detail, the parameters of the CCM vibration displacement system driven by a servo motor are shown in Table 1, which are mainly the parameters of servo motor Siemens 1FT6-134-6SB71.

TABLE 1. Technical parameters of servo motor

Physical parameters	Nominal value
Nominal power P_N	20.4 kW
Nominal current I_N	45 A
Nominal speed n_N	1500 r/min
Moment of inertia J	0.0547 N·m^2
Friction coefficient B	0.004 Nms/rad
Rotor flux linkage ψ_f	0.96 Wb
Pole pairs p	3
Equivalent inductance L	0.0046 H
Equivalent magnet-resistance Rs	0.14 Ω

In the d-q coordinate system of permanent magnet synchronous motor (PMSM), the PI controller structure of the speed-loop and current-loop is following

$$u_{PI} = K_P\left(e(t) + \frac{1}{\tau_I}\int_{t_0}^{t} e(\tau)d\tau\right) \tag{59}$$

where u_{PI} is the control input, K_P is the proportional coefficient, and τ_I is the integration time. After parameters self-tuning by Siemens servo driver SINAMICS120 in the experimental field, the parameters of speed-loop controller and current-loop controller in Formula (59) are $K_{Pn} = 23.553$, $\tau_{In} = 10$ ms, $K_{PI} = 19.31$, and $\tau_{II} = 2$ ms, respectively. In [3], the parameters of the second-order oscillation link in Formula (1) are $K = 1$, $T = 0.0177$, $\xi = 0.707$.

The parameters of the proposed control strategy are chosen as $\alpha_1 = 1$, $\beta_1 = 4$, $\mu = 0.02$, $k_m = 5$, $\rho = 1$, $\vartheta = 5$, $\varphi = 80$, $c_1 = 35000$, $c_2 = 10000$, $c_3 = 300$, $l = 0.75$.

The non-sinusoidal vibration curve of the CCM is Demark curve [1], which is selected as

$$s_{pd} = h\sin(\omega t - A\sin(\omega t)) \tag{60}$$

where $h = 3$ mm, $\omega = \frac{2\pi}{60}f$, f is the CCM vibration frequency and $f = 90$ time/min. The deflection rate is $\alpha = 0.24$, $A = \pi\alpha \big/ \left(2\sin\left(\frac{\pi}{2}(1+\alpha)\right)\right)$.

In addition, the initial deviation of the mechanical zero position of the eccentric shaft at the initial time is taken as $d_1 = -0.25$ rad. Moreover, the varying-time load disturbance of the CCM vibration system [3] is

$$T_L(t) = [6.4985\sin(9.42t - A\sin(9.42t)) + 5.1335]\ \text{N·m} \tag{61}$$

Simulation results are shown from Figure 3 to Figure 6.

Figures 3(a) and 3(b) show the vibration displacement tracking curves and tracking error curves of the CCM with two different methods, respectively. In Figure 3(a), it can be seen that it enters a stable state after $t = 0.2$ s. Thus, both methods can achieve better tracking effect on the whole control process, but the PI control adjustment-time is slightly longer than the proposed method. In Figure 3(b), the proposed method has faster convergent speed, smaller overshoot and higher convergent accuracy than the PI control method.

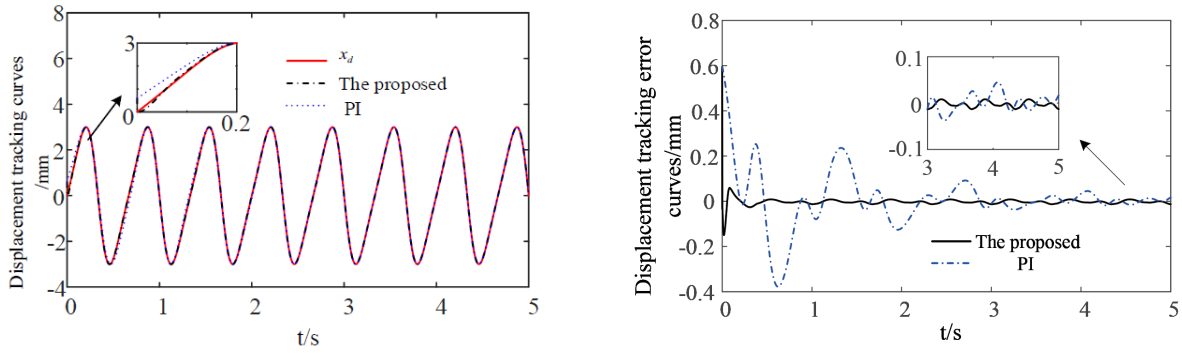

(a) Displacement tracking curve

(b) Displacement tracking error curve

FIGURE 3. Tracking curves of the control method proposed in simulation

Figure 4 shows the angular displacement and its tracking error curves of the eccentric shaft. It can be seen in Figure 4 that there is the overshoot at first, and then it quickly tracks the desired curve in finite time and its convergent speed is fast under the adaptive super-twisting SMC law. However, the overshoot of PI control is small, but the adjustment time is long, and there is steady-state error.

Figure 5 shows the speed response curve of the servo motor under two different methods. It is shown that the motor rotates at variable speed in one direction, which meets the requirements of the CCM process control constraints. In detail, the adjustment time of PI control method is slightly longer than the proposed method. Figure 6 shows the changing

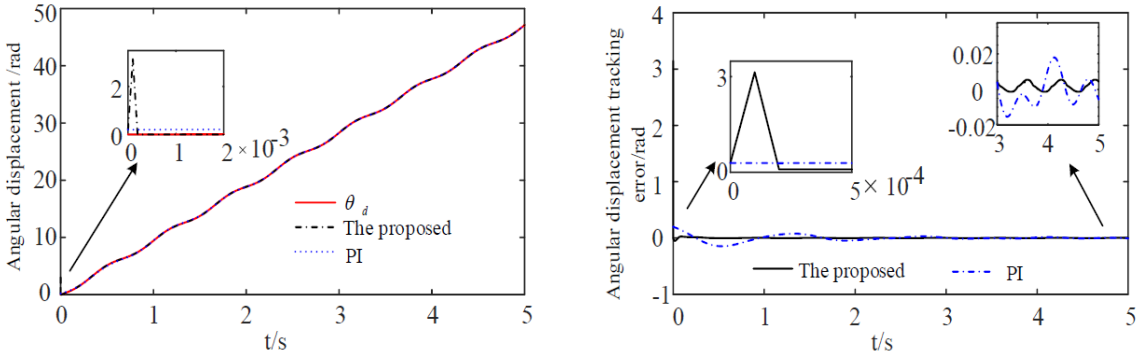

(a) Angular displacement tracking curve (b) Angular displacement tracking error curve

FIGURE 4. Angular displacement and tracking error curves of eccentric shaft

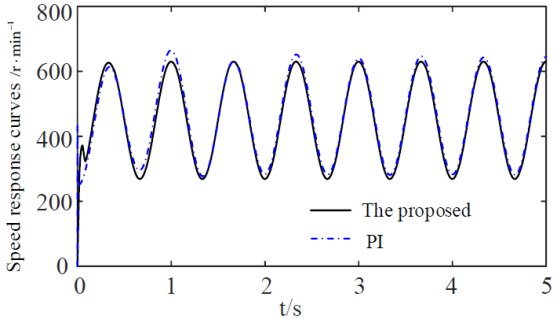

FIGURE 5. The speed curve of servo motor in simulation

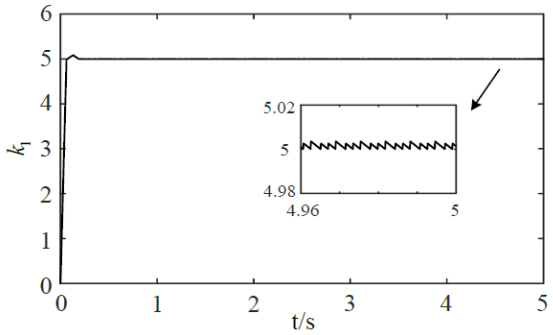

FIGURE 6. k_1 adaptive changing curve in simulation

curve of the adaptive controller parameter k_1. In Figure 6, it shows obviously that the k_1 is finally stable around 5.

4.2. **Experimental researches.** To further verify the effectiveness and application feasibility of the proposed control strategy in this paper, the simulation device of the CCM vibration displacement system driven by servo motor based on Siemens SIMOTION D425 and SINAMICS120 is used to complete the experimental verification, and it is shown in Figure 7. Furthermore, it mainly includes a simulated shaking platform, an electrical control cabinet of SIMOTION D425, an upper computer installed with a SCOUT system and a vibration displacement sensor, etc. In addition, SIMOTION D425 is the control center of the electrical control cabinet [27], which is a high-performance motion controller, and can realize motion control, logic control and process control at the same time. The upper

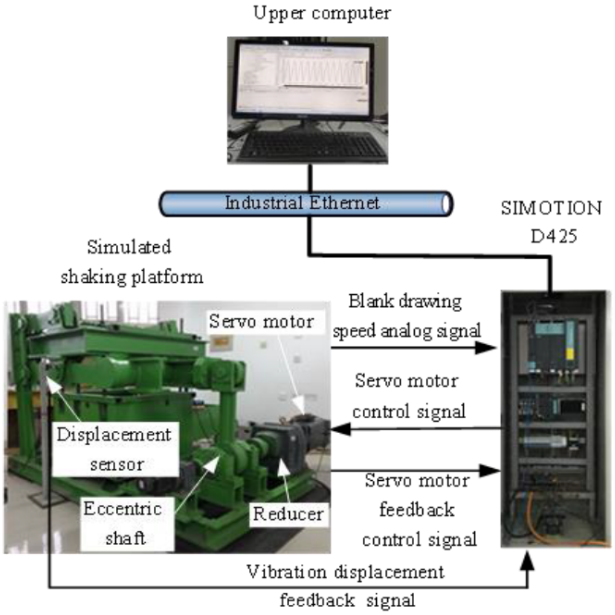

FIGURE 7. Experimental platform of CCM driven by servo motor

computer needs to install SCOUT software, which is programming and debugging special software, and can monitor and collect the real-time curves of each variable by using the tracing function.

In the experiment, the parameters selection of non-sinusoidal vibration waveform is the same as that of simulation. Since the mechanical initial zero position positioning is carried out in the first vibration cycle of about 0 to 2000 ms, the servo motor starts slowly, x_d is not loaded temporarily, and the displacement-loop controller does not work at this time. After the mechanical zero positioning being completed, x_d is given regularly, and the displacement-loop controller is enabled to carry out the closed-loop control of CCM vibration displacement. Finally, the experimental results are shown in Figure 8 to Figure 11.

Figure 8 and Figure 9 show the vibration displacement tracking curves and the tracking error curves of the PI control method and the proposed control method, respectively. In Figure 8, compared with the proposed control method in this paper, it can be seen that the adjustment time of PI control is longer and the overshoot is larger. In addition, the root mean square error and the relative error of PI control are 0.125 mm and 6.12%, respectively. In Figure 9, the adjustment time is short, the overshoot is small, the steady-state error is small, the root mean square error and the relative error of the proposed method are 0.104 mm and 5.05%, respectively.

Figure 10 shows the tracking curve of the servo motor speed. As can be seen in Figure 10, the servo motor rotates with variable speed in one direction, and it can completely satisfy the operational requirements of the process control constraints of the mechanical device.

Figure 11 shows the k_1 adaptive curve in the experiment. It is seen that k_1 is different from the simulation adaptive curve in Figure 6. The main reason is the difference between the actual experimental and simulation environment, which also verifies and fully shows the advantages of the adaptive control system.

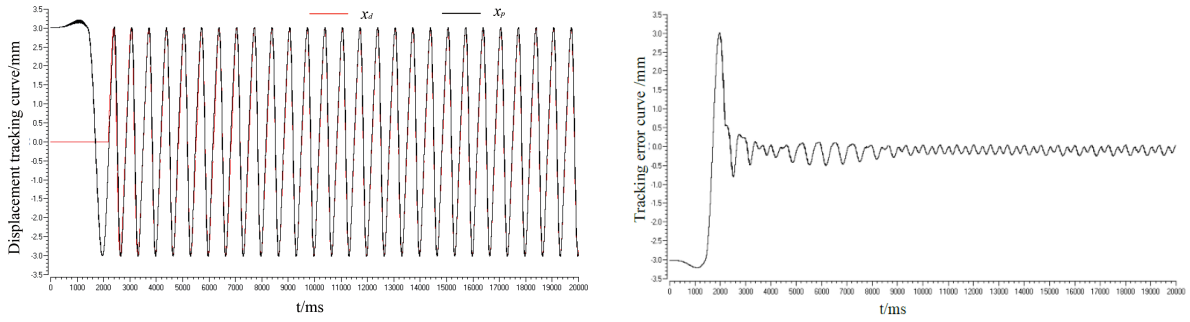

(a) Displacement tracking curve (b) Displacement tracking error curve

FIGURE 8. Tracking curves of the PI control method in experiment

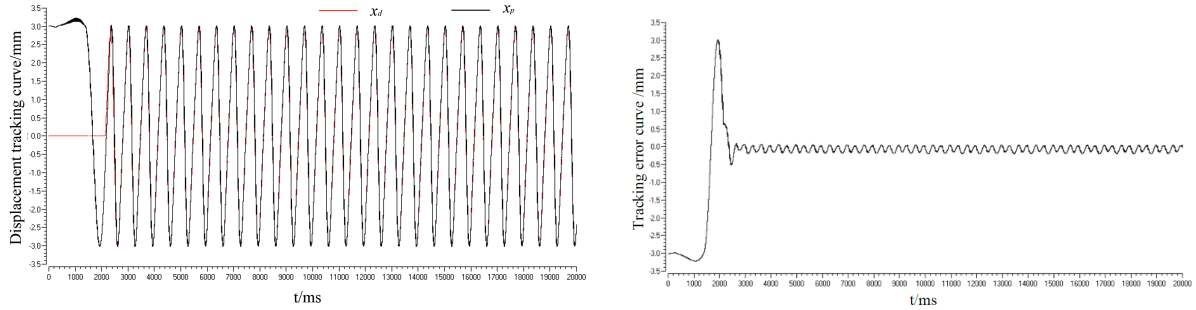

(a) Displacement tracking curve (b) Displacement tracking error curve

FIGURE 9. Tracking curves of the proposed control method in experiment

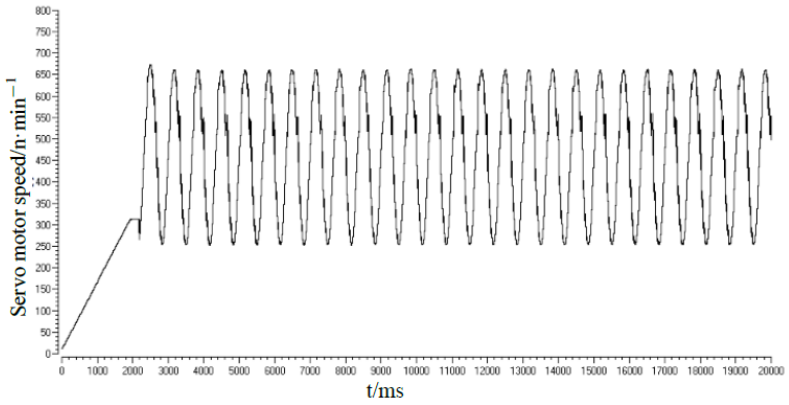

FIGURE 10. The speed curve of servo motor in experiment

5. **Conclusions.** In this paper, to improve the tracking control accuracy of the CCM vibration displacement system, an adaptive super-twisting control strategy based on nonlinear processing method is proposed in view of non-unique problem of inverse solutions of nonlinear output function and unknown disturbances. During the controller design procession, the main contributions of this paper are as follows.

1) A new nonlinear processing method is designed to solve the non-unique problem of inverse solutions of nonlinear output function, which lays a foundation for designing controller.

2) To suppress the uncertainties and time-varying load disturbance in the CCM system, a super-twisting controller based on parameter adaptive is designed for the displacement

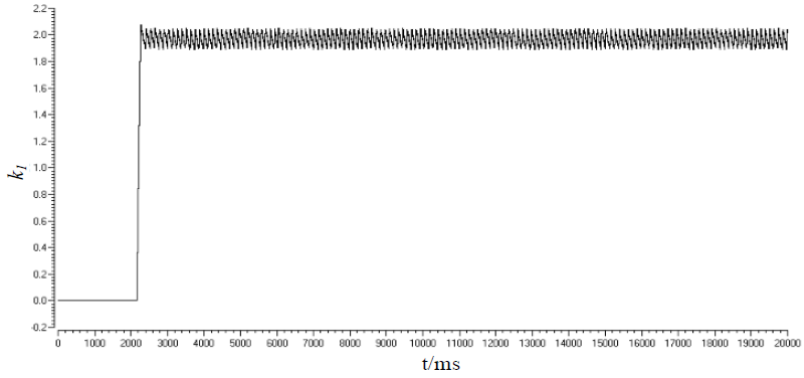

FIGURE 11. k_1 adaptive curve in experiment

loop, and it is proved that the tracking error of the CCM vibration displacement system is convergent in finite time by Lyapunov stability theory.

3) Compared with the PI control method in the field, the simulation and experiment of the vibration displacement system of the CCM are carried out. It shows that the proposed control strategy can accurately track the desired vibration displacement of the CCM in this paper. Meanwhile, the effectiveness and feasibility of the application of the proposed control strategy in practice also are verified, and it is easy to be applied to the actual engineering field.

In the future, the current research will be further extended to preset time control, while considering sensor and actuator failures of the continuous casting crystallizer vibration displacement system driven by servo motors.

Acknowledgment. This work is partially supported by the National Natural Science Foundation of China (61873226; 61803327) and Key Lab of Intelligent Data Information Processing and Control of Hebei Province, China and Science and Technology Plan Project of Tangshan. The authors also gratefully acknowledge the helpful comments and suggestions of the reviewers, which have improved the presentation.

REFERENCES

[1] K.-K. Cai, *Continuous Casting Mold*, Metallurgical Industry Press, Beijing, 2008.

[2] Y. Gan, H.-W. Tang and S.-T. Qiu, The role of continuous steel casting in the steel production process and an introduction to modern continuous casting technology, *Science in China (Series E: Technology Science)*, vol.38, no.9, pp.1384-1390, 2008.

[3] Y.-M. Fang, G.-Y. Li, J.-X. Li et al., Modeling and analysing for oscillation system of continuous casting mold driven by servo motor, *Chinese Journal of Scientific Instrument*, vol.35, no.11, pp.2615-2623, 2014.

[4] Z. Ma, Y.-M. Fang, J.-X. Li et al., Displacement tracking control for continuous casting mold driven by servo motor based on composite control strategy, *ISIJ International*, vol.60, no.4, pp.628-635, 2020.

[5] K.-S. Kang, L. Liu, Y.-M. Fang et al., Backstepping sliding mode control for continuous cast mold oscillation displacement system driven by servo motor, *Control Theory & Applications*, vol.33, no.11, pp.1442-1448, 2016.

[6] Q. Li, Y.-M. Fang, J.-X. Li and Z. Ma, Active disturbance rejection control for vibration displacement system of continuous casting mold driven by servo motor, *Electric Machines and Control*, vol.24, no.3, pp.147-156, 2020.

[7] Q. Li, Y.-M. Fang, J.-X. Li and H.-C. Zheng, Nonlinear processing for vibration displacement systems of contionus casting molds, *China Mechanical Engineering*, vol.30, no.12, pp.1433-1440, 2019.

[8] Z. Ma, Y. Fang, M. Xu et al., Finite-time tracking control of vibration displacement for continuous casting mold with control saturation, *Journal of the Brazilian Society of Mechanical Sciences and Engineering*, vol.44, no.1, pp.1-10, 2022.
[9] Z.-Y. Li, L.-Y. Yu, H. Liu et al., Nonlinear robust controller design for hypersonic vehicles, *Control Theory & Applications*, vol.33, no.1, pp.62-69, 2016.
[10] M. Yang, L. Niu and D.-G. Xu, Antiwindup design for the speed loop PI controller of a PMSM servo system, *Turkish Journal of Electrical Engineering & Computer Sciences*, vol.21, no.5, pp.1318-1327, 2014.
[11] X.-Y. He, X.-D. Li and S.-J. Song, Nonsingular terminal sliding-mode control of second-order systems subject to hybrid disturbances, *IEEE Transactions on Circuits and Systems II: Express Briefs*, vol.69, no.12, pp.5019-5023, 2022.
[12] P. Li, X. Yu and B. Xiao, Adaptive quasi-optimal higher order sliding-mode control without gain overestimation, *IEEE Transactions on Industrial Informatics*, vol.14, no.9, pp.3881-3891, 2018.
[13] F. Yong, F. Han and X. Yu, Chattering free full-order sliding-mode control, *Automatica*, vol.50, no.4, pp.1310-1314, 2014.
[14] B.-X. Ma and Y.-F. Wang, Adaptive high-order sliding mode control for oxygen excess ratio of PEMFC system, *Control Theory & Applications*, no.2, pp.253-264, 2020.
[15] T.-Q. Wang, B. Wang, Y. Yu et al., High-order sliding-mode observer with adaptive gain for sensorless induction motor drives in the wide-speed range, *IEEE Transactions on Industrial Electronics*, vol.70, no.11, pp.11055-11066, 2023.
[16] Z.-H. Zhao, D. Cao, J. Yang et al., High-order sliding mode observer-based trajectory tracking control for a quadrotor UAV with uncertain dynamics, *Nonlinear Dynamics*, vol.102, no.4, pp.1-14, 2020.
[17] X. Liu and W. Wang, High order sliding mode and its application on the tracking control of piezoelectric systems, *International Journal of Innovative Computing, Information and Control*, vol.4, no.3, pp.697-704, 2008.
[18] A. Chalanga, S. Kamal, L. M. Fridman et al., Implementation of super-twisting control: Super-twisting and higher-order sliding-mode observer-based approaches, *IEEE Transactions on Industrial Electronics*, vol.63, no.6, pp.3677-3685, 2016.
[19] K. Zhang, R. Xu, D. Kong, Q. Guan, X. Shen and J. Liu, Deadbeat predictive current control of permanent magnet synchronous motors with super twisting sliding mode observers, *ICIC Express Letters*, vol.17, no.6, pp.695-700, 2023.
[20] M. Gong, D. Zhou and X.-G. Zou, Saturated super-twisting sliding mode missile guidance, *Chinese Journal of Aeronautics*, vol.35, no.10, pp.292-300, 2022.
[21] Y.-K. Sun, W.-W. Lin, Y. Yuan et al., Direct torque control based on second order sliding mode for bearingless switched reluctance motor, *Electric Machines and Control*, vol.22, no.10, pp.67-76+86, 2018.
[22] Y. Shtessel, M. Taleb and F. Plestan, A novel adaptive-gain super-twisting sliding mode controller: Methodology and application, *Automatica*, vol.48, no.5, pp.759-769, 2012.
[23] X.-P. Lin, B. Zhang, S.-X. Fang et al., Adaptive generalized super twisting mode control for PMSMs with filtered high-gain observer, *ISA Transactions*, vol.138, pp.639-649, 2023.
[24] J.-B. Hu, X. Zhang, D. Zhang et al., Finite-time adaptive super-twisting sliding mode control for autonomous robotic manipulators with actuator faults, *ISA Transactions*, vol.144, pp.342-351, 2024.
[25] P. Sun, B Zhu, Z. Y. Zuo et al., Vision-based finite-time uncooperative target tracking for UAV subject to actuator saturation, *Automatica*, vol.130, 109708, 2021.
[26] H. Q. Wang, X. P. Liu, X. D. Zhao et al., Adaptive fuzzy finite-time control of nonlinear systems with actuator faults, *IEEE Transactions on Cybernetics*, vol.50, no.5, pp.1786-1797, 2020.
[27] W. Wang, *Simple Siemens Motion Controller: SIMOTION Practical Manual*, Metallurgical Industry Press, Beijing, 2013.

Author Biography

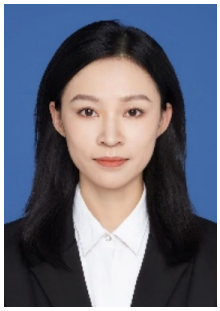

Na Yuan received the B.Sc. degree in Automation from the School of Electronic Engineering, Heilongjiang University in 2011 and a Master's degree in Control Science and Engineering from Hebei University of Technology in 2014. She is currently a Lecturer with the Intelligence and Information Engineering College, Tangshan University, Tangshan. Her research interests include nonlinear control, intelligent control and graphic image processing.

Zhuang Ma received the B.E. degree in Electrical Engineering from Southwest Jiaotong University, in 2001, and the M.E. and the Ph.D. degrees in Control Science and Engineering from University of Science and Technology in 2009 and Yanshan University in 2023, in China, respectively. He is currently a Professor with the Intelligence and Information Engineering College, Tangshan University, Tangshan. His research interests include nonlinear control, adaptive control, and system identification.

Jian Zhou received the B.E. degree in Mechanical and Electronic Engineering from Shandong Agricultural University in 2018 and the master's degree in Control Engineering from Yanshan University in 2021. He is currently an Electrical Engineer with Qingdao Gaoce Technology Co., Ltd. His research interest includes sliding mode control theory with applications to servo control systems.

Cheng Gong received the B.S. degree in Electrical Engineering and the M.S. and Ph.D. degrees in Control Science and Engineering from the Harbin Institute of Technology, Harbin, China, in 2002, 2004, and 2008, respectively. He is currently a Professor with the Intelligence and Information Engineering College, Tangshan University, Tangshan. His research interests mainly include stability analysis and stabilization for linear time-delay systems, H_∞ control, filtering and security for Markov jump systems, control for multi-agent systems, and integral inequality related to Lyapunov stability.